Finite size effects in diffusive public goods games

Philip Gerlee[1,*], Philipp M. Altrock[2]

1 Department of Mathematical Sciences, Chalmers University of Technology, Department of Mathematical Sciences, University of Gothenburg, Gothenburg, Sweden
2 Department of Integrated Mathematical Oncology, Moffitt Cancer Center and Research Institute, University of South Florida, Morsani College of Medicine, Tampa, FL, USA
***** Corresponding author: gerlee@chalmers.se

Abstract

A particular challenge in the co-evolutionary dynamics of growing populations is to determine the effects of population assortment on growth advantage of cooperative traits. Here we study the co-evolution of cooperators that are public good producers and consumers, and free riders that are only public good consumers. Using an individual-based model and its continuum limit we show that the differential growth rate between producers and free-riders depends on the spatial Fourier decomposition of their respective densities. Further, we derive a finite-size correction, which scales as the cell size, which accurately describes the dynamics of a randomly assorted population. Using this result we are also able to derive an effective benefit to cost relation, which provides a criterion that relates the parameters of the model (e.g. diffusion constant of the public good, decay rate and cost) to the long-term persistence of cooperation. Our findings provide a powerful tool for the analysis of diffusive public goods games, and can explain commonly observed patterns of cooperation, rather than the tragedy of the commons, based on the derived finite-size correction.

Introduction

Many organism are known to produce costly goods (e.g. molecules) that are released into the surrounding environment. These goods provide a benefit not only to producers themselves, but also to other surrounding organisms. Examples of this behavior range from microorganisms such as bacteria that release digestive enzymes [1] and siderophores that aid in the uptake of iron [2], to plants that release compounds that reduce herbivory [3], and beetles that produce pheromones that increase reproductive success [4]. Since public goods production comes at a cost, the resulting population dynamics can be seen as an evolutionary game.

Public goods (PG) games are also important in cancer biology. In evolving tumors growth factors (a type of hormone) typically produced by tumor associated cells (e.g. fibroblasts), have the ability to increase the rate of tumor growth [5, 6]. Recent findings in several different cancer models have shown that tumor cells have acquired the capability of producing growth factors which benefit themselves and neighbouring cells [7]. These examples include PDPG-production in brain cancer cells [8], Wnt-production in breast cancer [9] and testosterone-based interactions in prostate cancer cells [10].

These tumor cells typically harbor mutations that may lead to the production of a public good in form of a secreted factor. The fact that such production often comes at a fitness cost raises the question of how the production of a costly public good can be favored from an evolutionary perspective. The search for an answer to this question boils down to examining the relation between benefits and costs incurred by public good production. Only if the average benefit outweighs the cost producers can the producer type potentially spread in the population.

There have been several attempts to understand the problem of public good producer persistence in relation to the individual cost factor from a theoretical point of view. In an important set of experiments accompanied by mathematical modeling of an associated evolutionary public goods game [11], Archetti *et al.* showed that depending on external conditions either production or free-riding is favored. For intermediate background serum concentrations the two cell types could coexist, whereas a single type dominated in the case of low and high serum concentrations. This was explained using evolutionary game theory, as well as an individual-based (IB) model. The evolutionary game theory approach to the public goods game in evolving populations assumes a time scale separation between interaction and reproduction. The individual fitness values are calculated by averaging across all possible arrangements of cells [12, 13], which might be problematic as the actual size of the local group (or a distribution thereof) might be impossible to determine from experiment [11, 14]. The IB-model's strength in comparison to evolutionary game theory is that it does not assume averaging over possible cell arrangements. However, their model does not properly implement diffusion of the PG, but rather considers equal sharing of the PG within a certain radius on a Voronoi network.

An exact condition for when selection favors public good producers in a graph-based diffusible PG game was derived by Driscoll and Pepper [15]. Their scenario was similar to our IB-model and sought to capture the evolutionary game's dependence on the 'physics of diffusion'. The net benefit of PG production depends not only on the cost-to-benefit ratio, but also on the extent to which the PG is retained rather than distributed to neighboring cells. A potential drawback of such an approach is that the diffusion parameter on a graph does not necessarily have a direct physical meaning, but rather quantifies the amount of molecules that are transferred along edges of the population graph [16]. In the reality of *in vitro* and *in vivo* experimental models, the PG diffuses further than nearest neighbors and influences more distant organisms. This phenomenon would have to be captured by an alternative graph structure that cannot be determined ad hoc, and would require weighted links. Directly modeling diffusion based dynamics of public goods population dynamics might be the more feasible and bio-physical approach.

We here seek to understand how the physical parameters of the public good, e.g. the diffusion coefficient, the rate of good production, or the cost of production, affect co-evolution and co-growth of producers and free riders. We do not assume that the public good induces frequency-dependent selection or an implicit evolutionary game based on individual payoffs. Instead, we explicitly include production, diffusion and decay of the public good, as well as the spatial distribution of producers and free riders, in order to describe how these distributions change over time.

Model and Results

We seek to answer three basic questions about the coevolution of producer and free rider cells in an ecological context. First, we have been interested in how bio-physical parameters of public good availability and diffusion influence the intrinsic growth rates of cells. Public good production and diffusion and the characteristic distance between cells can be important factors that determine the fate of coevolving producers and free riders.

Second, we have sought to quantify the differential growth rate as a measure of success in the short-term, as well as its ability to predict long-term coevolutionary dynamics. As *in vitro* essays are often used to sequentially expand population and measure fitness differences, we wanted to find out whether and how initial condition and short-term success translate into long-term evolutionary outcomes.

Third, we have been interested in the roles of cellular dispersal and the cost of public good production. These

Table 1: Model parameters and variables (output observables)

Symbol	Meaning
α	Baseline cell division rate
κ	Cost of producing public good (public good)
μ	Rate of cell death
λ_c	Producer (cooperator) cell growth rate $\lambda_c = \alpha(1 + g(x,t)) - \kappa$
λ_r	Non-producer (free rider) cell growth rate $\lambda_r = \alpha(1 + g(x,t))$
δ	public good (public good) decay rate
ρ	public good (public good) production rate
D	public good (public good) diffusion rate
Γ	Cellular dispersal rate
$g(x,t)$	public good (PG) concentration
$c(x,t)$	Density of producer cells (cooperators)
$r(x,t)$	Density of free rider cells (free riders)
N_c, N_r	Total numbers of producer (cooperator, C), free rider (free rider, R) cells
q_n	Wave number ($q_n = 2\pi n$, n integer), used to describe fluctuations on different spatial scales
s	Average normalised cell density
N	number of lattice sites, inversely proportional to cell size $L = 1/N$

two cell type-specific quantities could vary significantly with the specific natural or experimental setting, and in particular with variations in cell size that in turn influences the distribution of cells. Overall, we seek to find analytical predictions that can quantify under which conditions cooperation in form of producer cells could prevail. Key observables of our model are the concentration of public good (PG), cellular densities of PG producer and free rider cells, as well as a description of how the densities fluctuate at different spatial scales, which can be captured with Fourier coefficients for different wave numbers (Table 1).

Continuum limit approach

A general approach to model the co-evolution of the two different cell types would be through an individual based approach on the level of cells, hybridized with a continuous description of PG dynamics, as shown in the Methods. However, immediate insights from individual based modeling can be difficult to obtain [17]. Thus, next to numerical simulations of a hybrid individual based model, we considered the following continuum approximation to describe the dynamics of the cellular densities in space and time, in the limit of negligible cell size (see Supplemental Methods):

$$\begin{aligned}\frac{\partial c(x,t)}{\partial t} &= \Gamma\left((1-r)\frac{\partial^2 c}{\partial x^2} + \frac{\partial^2 r}{\partial x^2}c\right) + \lambda_c(g(x))c - \mu c \\ \frac{\partial r(x,t)}{\partial t} &= \Gamma\left((1-c)\frac{\partial^2 r}{\partial x^2} + \frac{\partial^2 c}{\partial x^2}r\right) + \lambda_r(g(x))r - \mu r,\end{aligned} \tag{1}$$

where $c(x,t)$ denotes the density of producer cells and $r(x,t)$ the density of free riders (parameters are given in Table 1). A separation in time-scale between PG dynamics and cell division implies that we could assume the following stationarity condition for the PG concentration:

$$Dg''(x) + \rho c(x,t) - \delta g(x) = 0. \tag{2}$$

If such a time-scale separation is appropriate, the public good concentration will explicitly be driven by the dynamics of PG producer cells.

In order to quantify how cooperators fare over time, we considered the differential growth rate with respect to changes in the total numbers of producer and free rider cells (Table 1 and Methods)

$$\Delta_c(t) = \frac{dN_c(t)}{dt} - \frac{dN_r(t)}{dt}. \tag{3}$$

If $\Delta_c(t) > 0$ then producers grow at a higher rate than free riders and if $\Delta_c(t) < 0$ the opposite is true. It turns out that knowledge about the initial growth rate difference, $\Delta_c(0)$, is key in determining the overall fate of cooperators in the system. In an experiment, the differential growth rate corresponds to plating the cells at a given spatial density and measuring the change in the total number of producer cells and free rider cells over the course of a short period of time, e.g. over one cell cycle.

How can we approximate the initial growth rate difference in order to evaluate the short-term success of cooperators in the system? In the Supplementary Methods we prove a theorem that relates the differential growth rate to the parameters of the model in an exact way under specific geometric assumptions regarding the initial spatial distributions of producers and free riders. As a result, we find the following:

Theorem 1. *Assume that the initial densities $c(x,0)$ and $r(x,0)$ are both in $L^2(0,1)$. Then the differential growth rate of producer cells at time $t = 0$ is given by*

$$\begin{aligned}\Delta_c(0) = &\frac{\alpha\rho}{2}\sum_{n=1}^{\infty}\left(\frac{c_n^2 - c_n r_n}{\delta + Dq_n^2}\right)\\ &+ (\alpha - \mu - \kappa)c_0 - (\alpha - \mu)r_0\\ &+ \frac{\alpha\rho c_0^2}{\delta} - \frac{\alpha\rho c_0 r_0}{\delta}\end{aligned} \tag{4}$$

where $q_n = 2\pi n$, and c_n and r_n are the coefficients of the cosine Fourier series of $c(x,0)$ and $r(x,0)$ respectively.

This rather complicated expression simplifies if we consider fluctuations in a single wave number.

Corollary 1. *If the initial producer density is $c(x,0) = s + s\cos(2\pi n x)$ and the initial free rider density is $r(x,0) = s - s\cos(2\pi n x)$, with some constant amplitude $0 < s < 1$, then the differential growth rate at $t = 0$ is given by:*

$$\Delta_c(0) = \frac{\alpha\rho}{\delta + D\,(2\pi\,n)^2}\,s^2 - \kappa\,s. \tag{5}$$

This elegant result states that the growth rate differential is a linear function of the cost of PG production and its production rate, and establishes a reciprocal relationship to both the PG diffusion constant and the wave number, which describes the scale of spatial oscillation (Figure 1 E). A key assumption underlying the proof of this relationship is that the initial cellular densities can be represented as Fourier series on the unit interval. We compared the prediction of the model approximation in the continuum limit, Eq. (5), to stochastic simulations of the individual based model and found very good agreement (Figure 1 E).

The technical assumption that the initial cellular densities vary periodically in space appears to be a strong restriction. Hence we asked how a random initial condition would compare to the analytical prediction under such

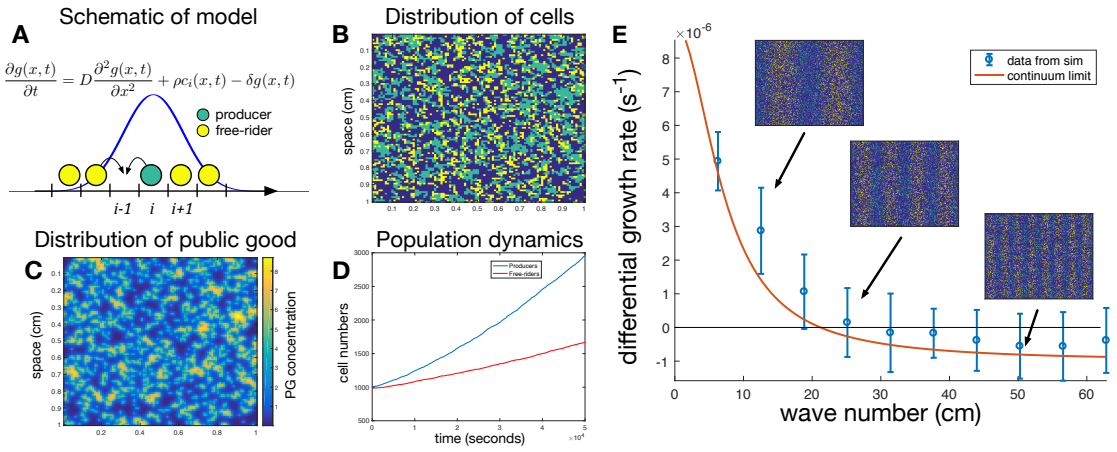

Figure 1: (A) Schematic of the individual-based model with a diffusible public good public good g. Cells are located on a lattice and can be of two types: producers cells that produce the diffusible public good, and free riders that do not produce but still receive benefit in the form of increased rate of cell division. The public good is produced at rate ρ, diffuses with diffusion constant D and decays at a constant rate δ. A possible concentration in space is given as the solid line–concentration spikes near producer cells. (B) In a typical simulation of the model the cells divide and place their offspring at neighboring lattice sites. This changes the spatial distribution public goods concentration (shown in C), which in turn affects the growth curves of the two cell types (shown in D). (E) The differential growth rate at time $t = 0$, where the initial density of producer and free riders oscillates in space with a wave number $q_n = 2\pi n$. The solid curve corresponds to the theoretical prediction (5). Note that the differential growth rate decreases with the wave number: producers grow at a slower rate when spatial dispersal has shorter characteristic length. Parameter values were set to $\alpha = 10^{-5}$ s^{-1}, $\kappa = 10^{-6}$ s^{-1}, $\rho = 10^{-3}$ s^{-1}, $\delta = 10^{-4}$ s^{-1} and $D = 10^{-6}$ cm^2/s. PG: public good.

seemingly narrow assumptions. In Figure 2 we show that even for a random initial condition we recover that the differential growth rate decays as $1/D$ with increasing PG diffusion constant. In addition, we computationally verified that $\Delta_c(0)$ increase linearly with PG production rate, and decreases linearly with increasing cost of PG production. The remarkable suitability of the analytic result (5) to predict differential growth rates of random initial conditions leads to the question whether cell size and cell count can be related analytically to the initial differential growth rate. This in turn would make it possible to observe differential growth for a specific set of cells in a public good setting, and then infer important parameters, such as the PG diffusion constant, or the PG production and decay rates.

Calculating the expected differential growth rate under stochastic initial conditions

We next calculated the expected differential growth rate for arbitrary stochastic initial cellular distributions. We convinced ourselves that stochastic, totally uncorrelated initial cellular distributions are realistic if the cell types were subject to a well-mixed solution before plating occurred. Such an initial condition will then lead to a maximally homogenous distribution in space. This scenario implies that the initial densities are constant in space, $c(x, 0) = c_0$ and $r(x, 0) = r_0$, for some positive constants c_0 and r_0. Consequentially, all other Fourier coefficients would be zero. In this case, the result (4) tells us that the differential growth rate should be independent of the diffusion coefficient D, as well as of the PG production and decay rates ρ, δ. However, this parameter independence is not what we observe in the stochastic individual based simulations with initially homogenous distributions of cells in space. Instead, the *expected* initial growth rate differential, after stochastic plating, resembles the form of the deterministic approximation (5). This behavior is explained by the following theorem, which describes random plating:

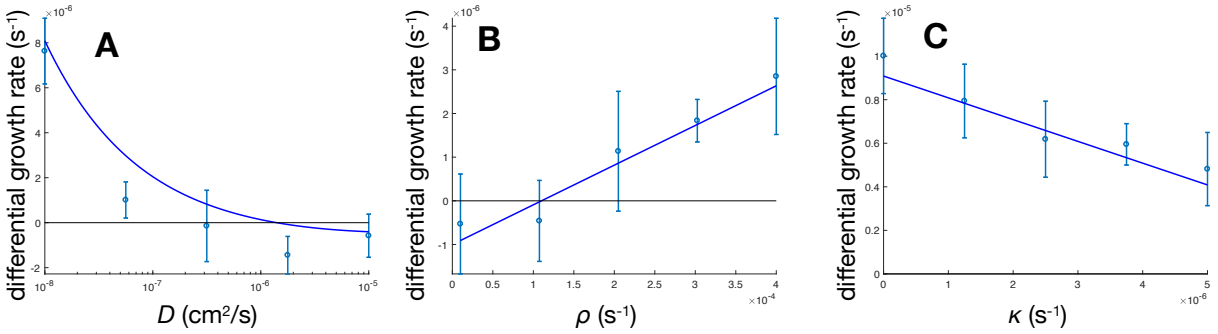

Figure 2: The differential growth rate at time $t = 0$ for a random initial condition with occupation probability $p_C = p_D = 0.1$. The circles show data from simulations (error bars corresponding to one standard deviation) and solid lines show the approximate theoretical prediction (7). (A) Shows the dependency on the diffusion coefficient of the public good, (B) the production rate of the public good and (C) the cost of production. The baseline parameters in all simulations were set to $\alpha = 10^{-5}$ s^{-1}, $\kappa = 10^{-6}$ s^{-1}, $\rho = 10^{-4}$ s^{-1}, $\delta = 10^{-4}$ s^{-1} and $D = 10^{-8}$ cm^2/s.

Theorem 2. *Assume that the initial condition to system (1) is given by two dependent Bernoulli processes (Suppl. Methods), where p is the occupation probability on the lattice. Then the expected differential growth rate of producer cells is given by*

$$\mathbb{E}[\Delta_c(0)] = \frac{\alpha\rho}{N}\, p \sum_{n=0}^{\infty} \frac{1}{\delta + D(2\pi\, n)^2} - p\,\kappa + \mathcal{O}\left(\frac{1}{N^3}\right) \tag{6}$$

where N is the total number of lattice sites, which is inversely related to the cell size.

A more general version of this result, with a cell type specific Bernoulli processes, is proven in the Supplementary Methods. The proof follows from a stochastic extension of Theorem 1.

For realistic parameter regimes, we expect that the PG diffusion constant is much larger than its decay rate, $D \gg \delta$, and we can approximate the infinite sum and find

$$\mathbb{E}[\Delta_c(0)] \approx \frac{\alpha\rho}{N}\, p \left(\frac{1}{2\delta} + \frac{1}{4\sqrt{\delta D}}\right) - p\,\kappa \tag{7}$$

Again, the differential growth rate has the form of a benefit minus a cost, but the benefit scales as one over the number of lattice sites, which is proportional to the cell size ($L = 1/N$). The benefit vanishes in the limit of zero cell size, leaving the cost term $-p\,\kappa$ to dominate, which implies that the benefit should be interpreted as a finite size correction to the continuum result (Theorem 1). The $1/N$-term thus captures the intuitive notion that any producer cell senses a higher local concentration of public good. We tested this prediction by initializing the IB-model with constant occupation probabilities $p = 0.1$, and measured how the differential growth rate depends on the other model parameters. These results are shown in Figure 2, were we can see excellent agreement between the theoretical result and stochastic simulation.

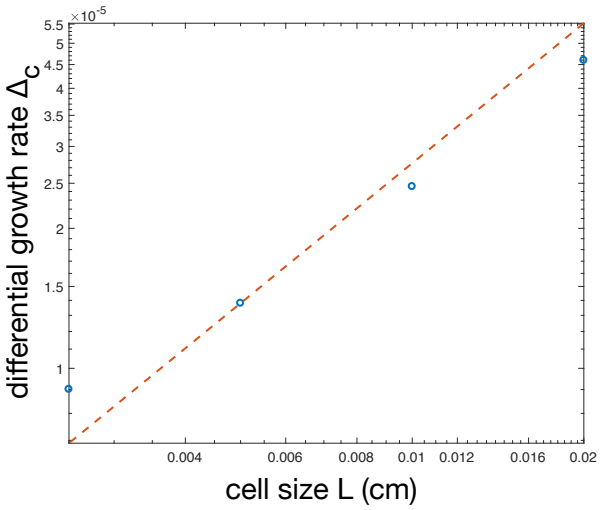

Figure 3: The differential growth as a function of the cell size $L = l/N$, where $l = 1$ cm is the domain size and N is the number of cells. The dashed line has slope 1 and shows that the differential growth rate scales as L, as predicted by our approximation of the form $\mathbb{E}[\Delta_c(0)] = \Delta_0 + \Delta_1 L$ (see Supplementary Methods).

Spatial variations in the density of cells can preserve the average benefit of public good production

We have shown that the finite size correction of the continuum model introduces a benefit to producers when the cell density is constant in space. Does this benefit persist on average if the density of cells varies in space? The following theorem provides a partial answer to this question.

Theorem 3. *Assume that the initial condition to system (1) is given by dependent Bernoulli processes with space-varying parameters* $p_c(x) = s + s\cos(2\pi n x)$ *and* $p_r(x) = s - s\cos(2\pi n x)$*, where* $0 < s < 1$ *and* n *is odd. Then the expected differential growth rate of producer cells is of the form:*

$$\mathbb{E}[\Delta_c(0)] = \Delta_0 + \frac{\Delta_1}{N} + \mathcal{O}\left(\frac{1}{N^3}\right) \tag{8}$$

whereby the first term is exactly given by (5), and $\Delta_1 \propto s(1-s)$ *(see Suppl. Methods).*

The equation (8) indeed states that there can be an average growth surplus for cooperators, under the assumption of stochastically varying initial distribution of cells of average size $L = 1/N$. In the non-zero cell size case, the expected differential growth rate can be viewed as the continuum result plus a positive finite size correction term of order L. We compare the analytic prediction with stochastic simulations of the IB model in Figure 3, which indeed shows that the benefit scales linearly with L.

Long-term dynamics

In a situation where cell migration occurs on a faster time scale compared to cell division, but is still slower than the dynamics of the public good, our previous results obtained in the case of randomly distributed of cells allows us to predict the long-term dynamics of the system. We explore this by considering a modified version of the

individual-based-model. Instead of placing the daughter cell in a neighboring lattice site, we instead pick a site uniformly at random in the entire spatial domain (a square lattice, for example). If the initial distribution of cells is random (see Suppl. Methods), and if daughter cells are dispersed uniformly at random, then the uncorrelated structure of the initial condition is preserved for all times.

The uncorrelated nature of cellular dispersal implies that we can interpret the expected growth rates of the IB model as the expected intrinsic per capita growth rates of producers and free riders. Let $c(t)$ denote the expected number of producer cells and $r(t)$ the corresponding quantity for free riders. Then we can formulate the following system of coupled ODEs [18]:

$$\begin{aligned}\frac{dc(t)}{dt} &= \Gamma_c(c)c(1-(c+r)) - \mu c \\ \frac{dr(t)}{dt} &= \Gamma_r(c)r(1-(c+r)) - \mu r\end{aligned} \tag{9}$$

where Γ_c and Γ_r are the per capita growth rates given by:

$$\begin{aligned}\Gamma_r(c) &= \alpha + \frac{\alpha\rho c}{\delta} - \frac{\alpha\rho cK}{N}, \\ \Gamma_c(c) &= \alpha + \frac{\alpha\rho c}{\delta} - \frac{\alpha\rho cK}{N} + \frac{\alpha\rho K}{N} - \kappa\end{aligned} \tag{10}$$

where

$$K = \frac{1}{2\delta} + \frac{1}{4\sqrt{\delta D}}. \tag{11}$$

Note that the two growth rates only differ by a constant, $\Gamma_c - \Gamma_r = \frac{\alpha\rho}{\delta N}K - \kappa$, which can be interpreted as the self-benefit to producer cells that scales with the cell size $L = 1/N$), minus the cost of production. An example for the dynamics of this system, in comparison to the population dynamics of the IB model, is shown in Figure 4 A, where the dashed lines correspond to the solution of Eq. (9) and the solid lines are obtained from the IB model. The overall behavior of the ODE-system is summarized in the following theorem.

Theorem 4. *The non-negative steady states of system (9) with growth functions (10) are given by*

1. *The empty state:* $(c_0, r_0) = (0, 0)$*, which is unstable if* $\alpha > \mu$
2. *The free-rider state:* $(c_1, r_1) = (0, \alpha - \mu/\alpha)$*, which is stable if* $\alpha > \mu$ *and* $\frac{\alpha\rho K(D,\delta)}{N} < \kappa$
3. *Producer state I:* $(c_2, r_2) = (\frac{a-b+\sqrt{E}}{2a}, 0)$*, which exists if* $E > 0$ *and* $\frac{a-b+\sqrt{E}}{2a} > 0$*, and is stable if* $\frac{\alpha\rho K(D,\delta)}{N} > \kappa$
4. *Producer state II:* $(c_3, r_3) = (\frac{a-b-\sqrt{E}}{2a}, 0)$*, which exists if* $E > 0$ *and* $\frac{a-b-\sqrt{E}}{2a} > 0$*, and is unconditionally unstable.*

The constants a*,* b*, and* E *are given by*

$$\begin{aligned}a &= \frac{\alpha\rho}{\delta} - \frac{\alpha\rho}{N}K \\ b &= \alpha - \kappa + \frac{\alpha\rho}{N}K \\ E &= (a+b)^2 - 4a\mu\end{aligned}$$

Note that the stability of the non-trivial steady states is mutually exclusive (state 2 vs. 3), which implies that only one non-zero stable state exists for a given set of parameter values.

It follows that in the long term, the competition between producers and free-riders depends on the sign of the quantity $\alpha\rho\, K/(N\,\delta) - \kappa$. If it is positive producers win out, and if it is negative free riders will dominate. If we consider this condition as a function of the diffusion constant, we can write the critical diffusion constant, below which producers dominate, as

$$D_{crit} = \frac{\alpha^2\rho^2\delta}{4(\alpha\rho - 2\,\delta\,\kappa\,N)^2} \tag{12}$$

This critical valus is shown in Fgure 4 B as a function of the cost κ, and shows that $D_{crit} \sim \kappa^{-2}$.

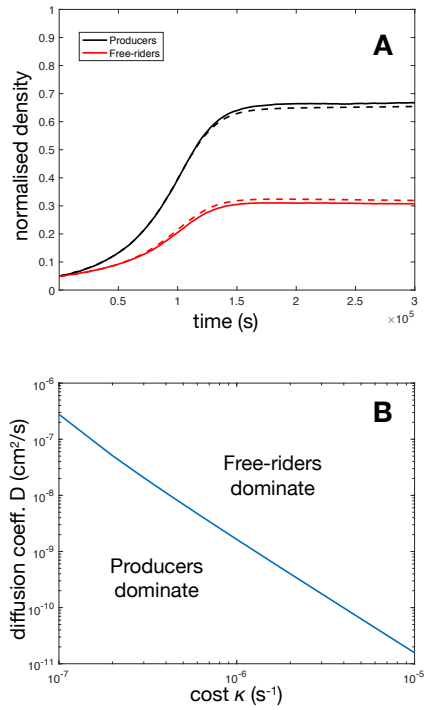

Figure 4: The dynamics of the IB-model with long-range dispersal. (A) Using our analysis of random seeding it is possible to predict the long-term dynamics of the individual-based model using the set of coupled logistic equations (10). The dashed lines correspond to the solution of Eq. (9) and the solid lines are obtained from the IB model simulations (Methods). (B) The dominance of one cell type over the other is determined by (12). The solid blue line shows the separation between these two regions in (D,κ)-space, and reveals that the critical diffusion coefficient scales as $D_{crit} \sim \kappa^{-2}$.

Discussion

We have investigated the dynamics of a population of organisms made up of two distinct types, producers that release a diffusible public good (PG) into the environment, and free riders that only reap the benefit of the PG. Starting with an individual-based model of the system we derived a set of coupled PDEs that describe how the densities of producers and free riders change in space and time. By analyzing these PDEs we could show that the

difference in growth rate between the two types can be expressed in terms of Fourier coefficients, highlighting that spatial oscillations impact the dynamics in a wave-length dependent manner. This approach also made it possible to obtain results for the case of a randomly distributed population, showing that producer cells obtain a benefit which depends on the cell size, effectively representing how much of the PG is retained by the cell itself. This finite size correction remains even when cell densities vary in space.

By considering a well-mixed version of the model we could show that the long-term dynamics is determined by the sign of the effective cost of cooperation

$$\frac{\alpha\rho K}{\delta N} - \kappa$$

If this quantity is positive then producers will outcompete free riders, whereas if it is negative the converse is true. This result is exact for the model with random dispersal, but also provides an upper bound for producer dominance. Even with no dispersal and limited cell migration, if $\alpha\rho K > \kappa N\delta$, producers will dominate. The reason for this is that random dispersal is the worst case scenario for producers, leading to maximum exploitation by free riders. If producers are allowed to aggregate, as is the case for zero dispersal and small migration rates, then the benefit they obtain from staying together is higher than the benefit to self seen in the case of dispersal. Thus, our prediction is that if the effective cost is positive, then producers will dominate independent of the migration rate.

In an experimental setting our theoretical predictions could be tested by measuring differential growth rates under varying conditions. For example one could vary the initial plating density of cells or alter the diffusion coefficient of the PG by altering the agar concentration.

One limitation of our model is that we consider public goods that are only subject to decay, and not consumption or uptake. Our assumption is certainly justified in certain cases such as enzyme production and pheromone release, since these compounds are not consumed by other organisms. However, our model also serves as good approximation for the case of uptake as long as the density of cells is approximately constant in space. Since in that case the uptake is also constant in space and can be approximated by a constant decay, albeit with a different rate constant that has to be adjusted for the average density in the system.

Our method is unable to capture how spatial correlations (or the relatedness parameter in the work if [15]) changes over time. This drawback can be avoided in two different ways. Firstly, it would be possible to keep the IB-model and make use of the technique developed in [18] and formulate equations not only of the average densities (i.e. eq. (10)), but also for the pair correlations between the cell types (three equations in total). A second approach would be to replace the IB-model with an off-lattice model and from that derive equations for the densities and pair correlations [19]. The latter approach would also make it easier to infer interaction strengths directly from time-course imaging data.

The discrepancy between results obtained from the IB-model and our theoretical predictions are mainly due to two factors. Firstly, we have assumed in our analysis of the IB-model that the separation in time scale between PG dynamics and cell division is complete. Although the separation is large ($\alpha/\delta \approx 0.1$), this assumption still introduces some error. Secondly, our analytical results are only correct to first order in $1/N$, which suggests that higher order terms (of order $1/N^3$) could be responsible for the observed discrepancies.

In conclusion we have presented and model of diffusible public goods and through mathematical analysis been able to predict the outcome based on the physical parameters of the system. Hopefully this will aid our understanding of evolutionary dynamics of cooperation in microbial system as well as in cancer.

Methods

In this section we describe the individual-based model, which have used for investigating the effect of a diffusing public goods in microbial populations. The continuum limit of the individual-based model and all theorems and proofs can be found in the Supplementary Methods.

Individual-based model

Let us consider a 2-dimensional spatial domain of linear size L, discretized into a lattice with $N \times N$ lattice points. The cells are located on this lattice, and each lattice point can be in three states: (i) contain a producer cell, (ii) a free rider cell or (iii) be empty. We index the lattice points with integers $i, j = 0, ..., N-1$ and denote the spatial distribution of producer cells with $c_{i,j}$, where $c_{i,j} = 1$ if a producer cell is located at (i, j) and zero otherwise. The free riders a denoted by $r_{i,j}$. Both cell types have the ability to divide, move and die, processes which will be described in detail below.

The discrete part of the model is coupled to continuous field which describes the public good's concentration, denoted $g(x, t)$. We assume that the public goods is produced by producer cells at some rate ρ, diffuses within the domain with diffusion coefficient D, and decays at a constant rate δ. This implies that the PG obeys the reaction-diffusion equation

$$\frac{\partial g(x,t)}{\partial t} = D\nabla^2 g(x,t) + \rho c(x,t) - \delta g(x,t) \tag{13}$$

where $c(x, t) = 1$ on lattice points that contain producer cells and $c(x, t) = 0$ otherwise. In order to accurately describe the dynamics within a confined domain, such as a Petri dish, we impose zero-flux boundary conditions on $g(x, t)$, i.e. $\nabla g(x, t) \cdot \mathbf{n} = 0$, where $\mathbf{n}$ is the normal vector of the boundary.

The public goods is assumed to affect the rate of cell division of both cell types in an identical fashion and for simplicity we assume a linear relationship between PG concentration and division rate. This implies that the division rate of a free rider cell located at position x is given by $\lambda_r = \alpha(1 + g(x, t))$, where α is the baseline rate of division. Producer cells have the same rate of division, but also pay an additional cost κ, which means that the rate of division for a producer cell located at x is given by $\lambda_c = \alpha(1 + g(x, t)) - \kappa$. Upon cell division a neighboring lattice point (using a von Neumann neighborhood) is chosen uniformly at random. If the lattice point is empty the daughter cell is placed there, but if it is occupied cell division fails.

The cells move between lattice points at a rate ν, which is equal for both cell types. When movement has been initiated a neighboring lattice point is chosen uniformly at random. If the lattice point is empty the cell moves to this new position, but if it is occupied movement fails.

Lastly cell death occurs at a constant rate μ, and leads to the instant removal of the cell from the lattice.

Numerical implementation

We consider a domain of size $l = 1$ cm, discretized into $N = 200$ lattice points, which yields a cell size of $h = 50$ μm. A simulation of the model is initialized by first prescribing the initial condition for the cells and the PG. Typically we consider a stochastic initial condition of the following form

$$\begin{aligned}
\Pr(c_{i,j} = 1 \text{ and } r_{i,j} = 0) &= f_c(ih, jh) \\
\Pr(c_{i,j} = 0 \text{ and } r_{i,j} = 1) &= f_r(ih, jh) \\
\Pr(c_{i,j} = 0 \text{ and } r_{i,j} = 0) &= 1 - f_c(ih, jh) - f_r(ih, jh) \\
\Pr(c_{i,j} = 1 \text{ and } r_{i,j} = 1) &= 0
\end{aligned}$$

where $i = 0, ..., N-1$ and f_c and f_r are functions from $[0, 1] \times [0, 1] \to [0, 1]$ prescribing the average initial density of cells. The domain is assumed to be void of PG corresponding to an initial condition of the form $g(x, 0) = 0$ for all $x \in [0, 1] \times [0, 1]$.

Time is discretized with a time step of $\Delta t = 10^2$ seconds, and each time step $n = 1, ..., t_{max}$ the following is carried out:

1. The equation for the PG concentration (13) is solved numerically using an ADI-scheme [20] with space step h and time step Δx, which yields the current concentration $g(ih, jh, n\Delta t)$ at all lattice points (i, j).

2. All the cells are updated in random order according to the steps:

   (a) A cell at lattice site i divides with probability $\alpha(1+g(ih, n\Delta t))\Delta t$ if it is a free rider or $(\alpha(1+g(ih, n\Delta t))-\kappa)\Delta t$ if it is a producer cell.

   (b) The cell moves with probability $\nu\Delta t$

   (c) The cell dies with probability $\mu\Delta t$.

The simulation is terminated when t_{max} steps have been carried out.

References

[1] Cavaliere M, Feng S, Soyer OS, Jiménez JI (2017) Cooperation in microbial communities and their biotechnological applications. *Environmental Microbiology* 19(8):2949–2963.

[2] Cordero OX, Ventouras LA, DeLong EF, Polz MF (2012) Public good dynamics drive evolution of iron acquisition strategies in natural bacterioplankton populations. *Proceedings of the National Academy of Sciences* 109(49):20059–20064.

[3] Dicke M (1999) Evolutionary patterns and mechanisms in consumer-resource interactions. *Journal of Evolutionary Biology* 12(2):419–420.

[4] Borden JH, Pureswaran DS, Lafontaine JP (2008) Synergistic blends of monoterpenes for aggregation pheromones of the mountain pine beetle (coleoptera: Curculionidae). *Journal of Economic Entomology* 101(4):1266–1275.

[5] Marusyk A, et al. (2014) Non-cell-autonomous driving of tumour growth supports sub-clonal heterogeneity. *Nature* 514:54–58.

[6] Altrock PM, Liu LL, Michor F (2015) The mathematics of cancer: integrating quantitative models. *Nature Reviews Cancer* 15:730–745.

[7] Tabassum DP, Polyak K (2015) Tumorigenesis: It takes a village. *Nature Reviews Cancer* 15:473–483.

[8] Heldin CH (2013) Targeting the pdgf signaling pathway in tumor treatment. *Cell Communication and Signaling* 11(1):97.

[9] Cleary AS, Leonard TL, Gestl SA, Gunther EJ (2014) Tumor cell heterogeneity maintained by cooperating subclones in Wnt-driven mammary cancers. *Nature* 508:113–117.

[10] Zhang J, Cunningham JJ, Brown JS, Gatenby RA (2017) Integrating evolutionary dynamics into treatment of metastatic castrate-resistant prostate cancer. *Nature communications* 8(1):1816.

[11] Archetti M, Ferraro DA, Christofori G (2015) Heterogeneity for IGF-II production maintained by public goods dynamics in neuroendocrine pancreatic cancer. *Proceedings of the National Academy of Sciences USA* 112:1833–1838.

[12] Hauert C, Holmes M, Doebeli M (2006) Evolutionary games and population dynamics: maintenance of cooperation in public goods games. *Proceedings of the Royal Society B* 273:2565–2570.

[13] Archetti M (2013) Dynamics of growth factor production in monolayers of cancer cells and evolution of resistance to anticancer therapies. *Evolutionary applications* 6(8):1146–1159.

[14] Gerlee P, Altrock PM (2015) Complexity and stability in growing cancer cell populations. *Proceedings of the National Academy of Sciences USA* 112:E2742–E2743.

[15] Driscoll WW, Pepper JW (2010) Theory for the evolution of diffusible external goods. *Evolution* 64(9):2682–2687.

[16] Allen B, Gore J, Nowak MA (2013) Spatial dilemmas of diffusible public goods. *Elife* 2.

[17] Black AJ, McKane AJ (2012) Stochastic formulation of ecological models and their applications. *Trends in Ecology and Evolution* 27:337–345.

[18] Baker RE, Simpson MJ (2010) Correcting mean-field approximations for birth-death-movement processes. *Physical Review E* 82:041905.

[19] Murrell DJ, Dieckmann U, Law R (2004) On moment closures for population dynamics in continuous space. *Journal Of Theoretical Biology* 229(3):421–432.

[20] Press WH, Teukolsky SA, Vetterling WT, Flannery BP (1996) *Numerical recipes in C*. (Cambridge university press Cambridge) Vol. 2.